Versatile Sensor Node with Acoustic Data Communication Capabilities for FSAT Networks in Guided Wave-based Structural Health Monitoring Applications

OCTAVIO A. MÁRQUEZ REYES[1], FEDERICA ZONZINI[2], MASOUD MOHAMMADGHOLIHA[2], JOCHEN MOLL[1] and LUCA DE MARCHI[2]

ABSTRACT

Correct evaluation of structural integrity and the ability to predict the remaining useful life of structures is of critical importance in numerous applications, particularly for aerospace industry. The development of Structural Health Monitoring (SHM) systems and their integration into real-world structures has become a necessity to provide a robust and cost-effective solution for structural assessment. Normally structure inspection is done periodically after weeks or months. For machines such as aircrafts or trains, they are taken out of service for structural integrity evaluation. Indeed, one main advantage of modern SHM systems is the continuous, autonomous monitoring of structures, even during service. Therefore, dense networks of ultrasonic transducers are distributed over structures to perform reliable damage detection and localization. Unfortunately, powering these poses many challenges in terms of cabling and added weight, besides to long latency times if a single central processing unit is charged of managing all transducers in the network. To solve this issue, new systems rely on specialized sensor nodes (SNs) and transducers, such as frequency steerable acoustic transducers (FSATs), which offer inherent directional capabilities for data actuation/sensing. These SNs can drive high voltages and various types of signals to and from transducers conforming a SHM network. They also perform signal treatment tasks and lead communication protocols, such as on-off keying (OOK) or frequency shift keying (FSK), and even help identifying defective nodes within the network.

Given the specificities of the FSATs, a matching SN is required to ensure reliable data exchange, even in cases in which traditional radiofrequency-based wireless communication is not possible. In this contribution, we address this need by presenting the design, implementation and test of a new, lightweight and low-cost SN, capable of driving voltage signals as high as 60 Vpp and powering both: commonly used piezoelectric transducers and the more specialized FSATs, and perform communication tasks, using a regular 5V USB port as power source. With this SN, the weight, latency and cable complexity of regular sensor networks are addressed, while disclosing novel opportunities for a higher level of automation and, hence, safer embedded SHM systems for ultrasonic inspection.

[1]Goethe University Frankfurt, Max-von-Laue-Straße 1, Frankfurt 60438, Germany.
[2]University of Bologna, Viale del Risorgimento 2, Bologna 40136, Italy.

INTRODUCTION

Continuous Structural Health Monitoring (SHM) systems for aerospace, mechanical and civil structures have great potential for damage detection in service life assessment and failure prediction. These systems are often based on guided acoustic waves and their inherent ability to propagate long distances with minimal disruption, reliability in a variety of environments, and natural protection against electromagnetic interference. Data communication through structures using elastic ultrasonic guided waves (GWs) has become an attractive alternative. Lamb waves are of particular interest in this case, as recent works on data transmission [1], power [2] and defect imaging [3] have proven to be reliable, even against changing environmental conditions [4].

The central idea behind the use of GW for communication purposes, as shown in [2] and [5], is to simultaneously use the same elastic waves to test structural integrity and provide the results of the inspection itself. In addition, it was also established in [6] that Multiple-In Multiple-Out communication can be performed efficiently by cheap and low-power electronic devices using acoustic channels. However, the implementation of cable-based SHM systems in large structures suffers from the inability to locally process received data, the relatively high voltage required to drive transducers in the network, or sensing and control. Additional problems arise, such as implementing a separate system demanding use of additional cables or communication channels. In addition, data workload limitations due to extensive cabling must be taken into account [7]. The latter imposes additional costs [8] and power and weight requirements, as well as being difficult to maintain. However, certain sectors, such as the aerospace industry, cannot afford these additional costs [9], [10]. To address the above issues, many studies have explored the development of dedicated hardware that connects directly to sensors in the network. In fact, surveillance networks based on GW currently consist of piezoelectric transducer connected to embedded solutions capable of performing mixed-signal processing, triggering, and defect detection [5], [11], [12].

In this article, we propose a portable, light-weight and versatile sensor node for acoustic data communication and damage detection suited for the connection to various types of piezoceramic transducers.

SENSOR NODE DESCRIPTION

The sensor node (SN) developed in this work is design over a 4-layer PCB, carefully tailored to adapt perfectly to a STM32 Nucleo-144 board (figure 1). The SN can drive a wide plethora of transducers, from specialized frequency acoustic steerable transducers (FSATs) [13] as well as more commercial piezoceramic discs. The device was adapted to handle logic and analog low voltage (LV) from ±3.3 V to ±5 V as well as higher actuation voltages of about ±30 V (HV) and it is powered via a micro-USB connector. It contains three main modules: the first one is in charge of actuation, signal conditioning and piezoelectric transducers driving. A second block is designed for low power signal acquisition, filtering, and adaptation, and finally a third one implements power management. The functionality of the device is governed by a STM32L4P5 low power microcontroller (MC).

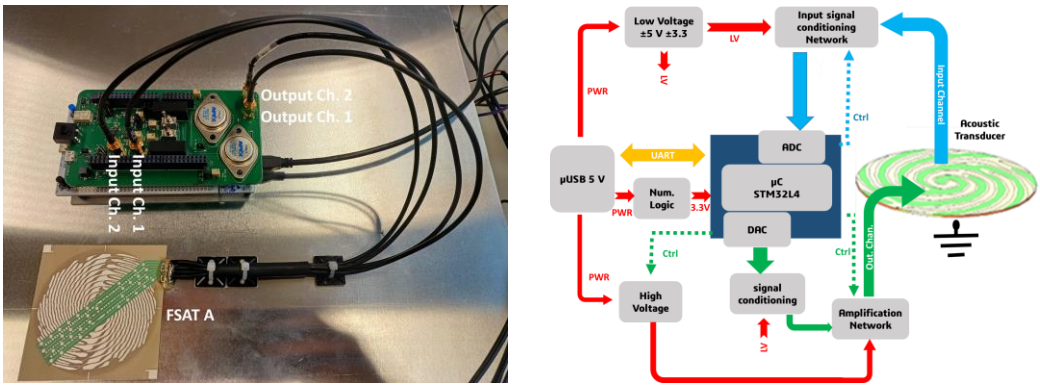

Figure 1. Left: Sensor Node connected to a FSAT. Right: elementary SN building blocks

The actuation module is based on two digital-to-analog converters (DAC) of the MC. A filter and amplification network, supported by the power management circuit, adjusts the DACs signals and send them through SMA Connector Jacks. The reception module starts with two independent channels attached to SMA Connector Jacks, each of them having an adjustable filter necessary to set the bandwidth to the frequency range of interest, hence enhancing the signal received by the sensors. The module enables gains of 1 to 10000 and performs offset compensation for adequate lecture of the MC's analog-to-digital converters (ADCs). The last module manages the power required for the SN, coming either from a direct source connected to the SN or the attached Nucleo board. The main electrical characteristics of the prototyped SN are given in table I.

Two different types of transducers were connected to the SN: the first one is a commercial omnidirectional ceramic DuraAct patch transducer, as used in [14]. The second one is a FSAT with 5 electrodes, corresponding to 4 channels for actuation-reception and common ground. To drive this transducer and to take advantage of its acoustic beamsteering capabilities, at least two of these channels need to be actuated simultaneously, either with two signals shifted 180° from each other or in quadrature. The radiation patterns for this kind of actuation is well depicted in [13], [15] and [16]. This leaves the remaining channels for reception as shown in figure 1.

TABLE I. SENSOR NODE CHARACTERISTICS

Parameter	Value	Dimensions
Main Power Source	5	V (µUSB)
Max. Output Amplitude	60	Vpp piezoceramic discs
Max. Output Amplitude	11	Vpp FSAT
Sampling frequency	5	Msps
Frequency range	up to 320	kHz
Actuation/ Reception channels	2/2	-
Dimensions	71 x 124	mm

EXPERIMENTAL SETUPS

For this study we tested the SN with two different types of transducers installed on the structures in figure 2. The first one (left) corresponds to a carbon fiber reinforced

plastic (CFRP) plate manufactured with quasi-isotropic layup. A network of 12 omnidirectional transducers has been attached over its surface. This particular plate was deeply studied and measured under various conditions with specialized equipment described in greater detail in [17]. All this data was stored in an open database providing the ideal test structure for comparison and validation of the measurements performed with our SN. The second structure (right) is an aluminum plate with a network of three FSATs deployed. The plates are placed over elastic foam to avoid vibrations or reflections coming from the surface below.

Damage Detection on the CFRP Plate with Omega Stringer

To validate the actuation and reception capabilities of SN, it was connected to the CFRP plate to repeat the same measurements performed in [17]. For our validation, we took a single transducer (T4) as actuator and transducers T7, T8, and T11 as receivers, in a pitch-catch configuration: the actuation frequencies were selected to be 40, 60 and 260 kHz. To actuate the piezoceramic transducers, T4 has been connected to output channel 1 of the SN, while input channel 1 was connected, time by time, to T7 (T8 or T11), as presented in figure 1. A five-cycle Hann-windowed sine signal was used for excitation as described in [17], with a voltage amplitude of 60 Vpp.

Defect detection capability was also investigated by employing a reversible damaging procedure: a cylindrical aluminum mass with diameter of 10 mm and height of 2 mm has been attached with tacky-tape to the CFRP plate surface, on the path between T4 and sensors T7 and T8 (as magnified by a yellow arrow in figure 2).

Communication Setup

Moreover, from a directional acoustic data communication point of view, we selected a single FSAT (FSAT A) as actuator while the other two, FSAT B and FSAT C, worked as receivers. Two SN (SN A and SN B) were employed for this task given the differential nature of the involved transducer: SN A acted as transmitter by implementing OOK data modulation bursts were transmitted at the specific frequencies relative to the directions of FSAT B and FSAT C.

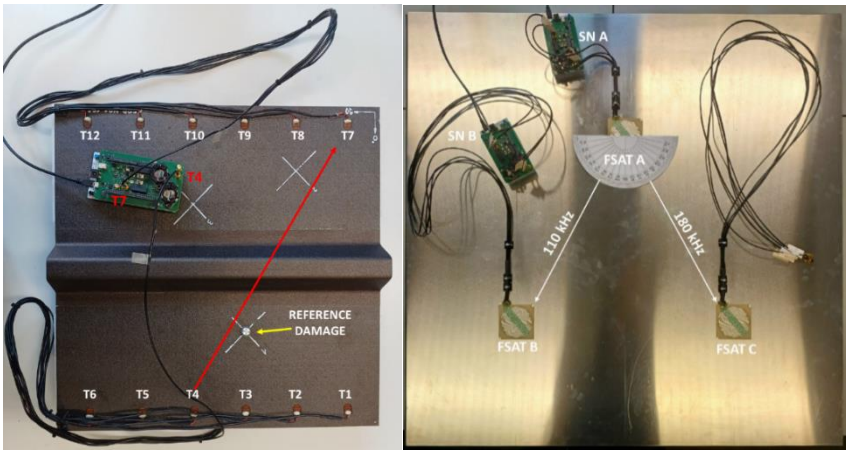

Figure 2. Left: CFRP plate with stringer, omnidirectional transducers and reference damage. Right: aluminum plate and communication setup between FSATs and expected transmission paths

The latter were connected, test-by-test, to a SN_B configured to work in receiver mode. The cycles of the Hann-windowed actuation signals were adapted in a way that they have a fixed duration of 100µs independently from the carrier frequency; the voltage amplitude was reduced and adapted to the higher capacitive load of the FSATs compared to piezoelectric discs. Figure 2 depicts the setup and the desired directions for the guided waves, while table III presents the plate characteristics and the communication parameters.

Additionally, FSAT A was also configured to actuate a signal given by the superimposition of tone bursts corresponding to the path from FSAT A to FSAT B (110 kHz) and the path from FSAT A to FSAT C (180 kHz). This MIMO-like test was necessary to assess the multipath communication performances of the designed custom electronics (SN and transducer). So at every end the expected message could be discriminated from additional parasitic frequencies. A sample of the actuation signals used during the experiments next to their spectrum is presented in figure 3: the power of the superimposed signal shows two clear peaks at the two selected spectral components. The superimposed signal was finally normalized to adjust to the load as its original components (110 kHz and 180 kHz), for this reason its spectrum only present half of the expected power after superposition of the two components.

TABLE II. EXCITATION SIGNAL PARAMETERS DAMAGE DETECTION

Signal Type	**Parameter**	**Value**
Tone burst	Center frequencies	40 kHz, 60 kHz, 80 kHz
	Number of cycles	5
	Windowing function	Hann
	Amplitude	~60 Vpp
	Number of measurements per frequency	200

TABLE III. EXCITATION SIGNAL PARAMETERS FSAT DATA COMMUNICATION

Signal Type	**Parameter**	**Value**
Single Frequency Tone burst	Center frequency	110 kHz
Single Frequency Tone burst	Center frequency	180 kHz
Multiple Frequency Tone burst	Center frequencies	110 kHz & 180 kHz
	Windowing function	Hann
	Amplitude	~11 Vpp
	Time span between bursts	2 milliseconds

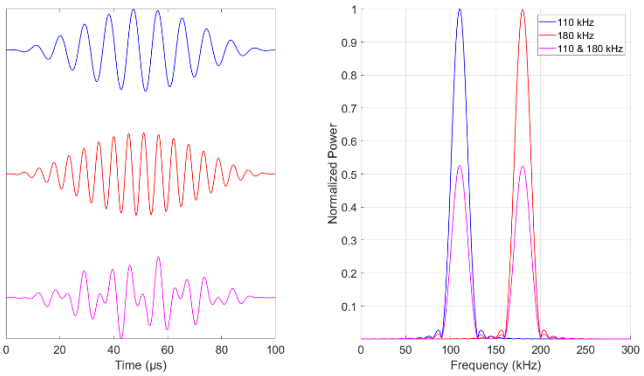

Figure 3. Depiction of employed multi-frequency tone burst. Left: Time-domain representation. Right: Spectral content of the waveforms.

RESULTS AND DISCUSION

The signals obtained with the pristine CFRP and the SN were compared with their respective counterpart obtained with a commercial Handyscope HS5 (TiePie Engineering) and a broadband amplifier PD200 (PiezoDrive Ltd, Shortland, NSW 2307, Australia) system stored in the Open Guided Wave (OGW) Datasets (http://openguidedwaves.de/) [17], providing a suitable fit of the results. One representative sample of this fitting for 40 kHz actuation is presented in figure 4.

After this initial validation, we performed SHM measurements in the pursuit of damage identification: 100 signals were taken for the CFRP plate with surface-mounted masses and compared with 100 signals of the pristine plate. The recovered wave signals were processed with the root mean square (RMS) metric resulting in a scalar value for each measurement point: figure 4 (right) displays an exemplary result for the detection of surface contaminants for actuation at 40 kHz and 5 cycles. The reference conditions can be distinguished from the contaminated conditions.

As for data communication, figure 5 shows results of GW-based communication between FSAT A to FSAT B and FSAT A to FSAT C, respectively: a stream of 10 bits is transmitted using OOK in frequency with a bit-rate of 0.5 kb/s. The communication approach based on the analysis of the spectral properties (frequency amplitude and location) of the received waves help to reduce the challenges arising from their inherent propagation behavior and additional complexity associated with multiple reflections.

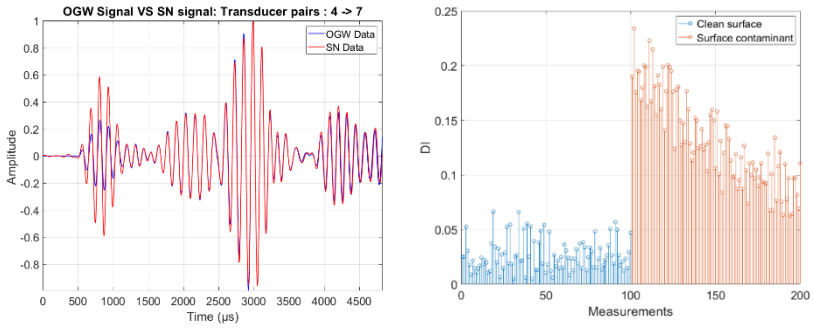

Figure 4. Left: Recovered signal SN and comparison with data from database pristine CFRP plate, 5-cycle actuation signal at 40 kHz. Right: Exemplary results for the detection of reference damage.

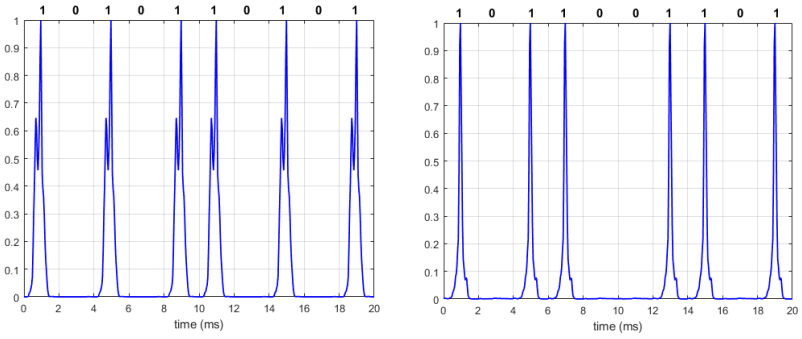

Figure 5. Exemplary results of 10 bits data communication. Left: FSAT A transmit m = [1010110101], 1 bit every 2 ms, FSAT B registers wave packets with reflections. A clear peak in the spectrum of the signal occurs after burst actuation, representing a “1”, signal close to zero, when only noise is registered represents a “0”. Right: FSAT A transmits FSAT C at 180 kHz m = [1011001101]

The transmission-reception procedure worked as follows: the SN actuates FSAT A to transmit a 10 bit message m = [1 0 1 0 1 1 0 1 0 1] ("1" corresponding to a single burst and the absence of it represents a "0") during a time window of 20 ms (every bit has a duration of 2 ms); this bit-rate has been chosen to avoid the problem of intra-bit interference upon reception, the bit stream is read by FSAT B with additional reflections from borders, and, hence, transformed to the frequency domain: a high peak occurs when a burst is actuated, while a significant reduction of its amplitude (more than 66%) indicates the reception of a digital "0". With this approach, we were able to successfully transmit two different messages within the FSAT network, establishing basic "directional" communication.

Furthermore, by performing the superposition of the previously tested excitation signals and performing actuation on FSAT A, we obtained the lectures from FSAT B and FSAT C presented in figure 6. From these spectra it can be seen that, although both spectral components are registered by both FSATs, less than 66% in the power of the secondary signal was acquired for both cases (i.e., of the carrier belonging to the different propagation direction) was measured, hence proving the directional capabilities of the transducer. These results show a clear discrimination of the signals frequency and direction, allowing the SN to perform individual directional and simultaneous communication by means of the spatial filtering capability of the FSAT.

CONCLUSION

The sensor node presented in this article was developed to have the flexibility to drive various types of acoustic transducers and enable the measurement and transmission of GWs within an acoustic SHM network. The device is powered by a common 5 V USB port and is capable to master relatively high voltage and perform damage detection over structures. Its versatility allows the SN to easily adapt to the connected type of transducer and the required signal by hardware and software. Finally, measurements performed over a characterized CFRP plate validate the use of the node for SHM applications. Moreover, tested with a small network of directional transducers, it aptness to perform directional and multipath data communication.

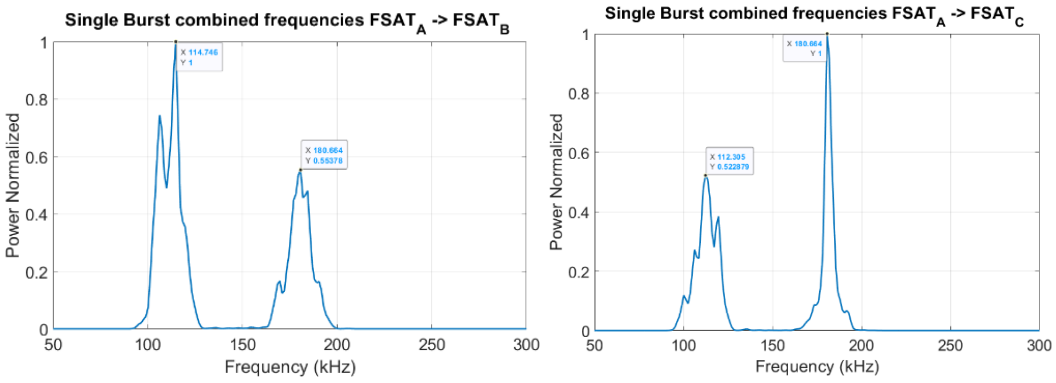

Figure 6. Received power at FSAT B (left) and FSAT_C (right) from multi-frequency tone burst actuation on FSAT_A

ACKNOWLEDGMENTS

OMR and JM gratefully acknowledge financial support by the German Research Foundation (DFG) under grant 349435502. FZ, MM and LDM gratefully acknowledge funding from the European Union's Horizon 2020 project Guided Waves for Structural Health Monitoring (GW4SHM, GA: 860104).

REFERENCES

1. I. Ahmed, H. Khammari, A. Shahid, A. Musa, K. S. Kim, E. De Poorter, and I. Moerman, "A survey on hybrid beamforming techniques in 5g: Architecture and system model perspectives," IEEE Communications Surveys & Tutorials, vol. 20, no. 4, pp. 3060–3097, 2018.
2. D. Headland, Y. Monnai, D. Abbott, C. Fumeaux, and W. Withayachumnankul, "Tutorial: Terahertz beamforming, from concepts to realizations," Apl Photonics, vol. 3, no. 5, p. 051101, 2018.
3. L. F. Ariza Vesga, "Many-objective problems optimization focused on energy efficiency applied to 5g heterogeneous cellular networks using the small cell switch-off framework," PhD dissertation, National University of Colombia, 2020.
4. W. Z. Khan, M. Rehman, H. M. Zangoti, M. K. Afzal, N. Armi, and K. Salah, "Industrial internet of things: Recent advances, enabling technologies and open challenges," Computers & Electrical Engineering, vol. 81, p. 106522, 2020.
5. C. Kexel, M. Mälzer, and J. Moll, "Guided wave based acoustic communications in structural health monitoring systems in the presence of structural defects," in 2018 IEEE International Symposium on Circuits and Systems (ISCAS). IEEE, 2018, pp. 1–4.
6. Y. Sun, Y. Xu, W. Li, Q. Li, X. Ding, and W. Huang, "A lamb waves based ultrasonic system for the simultaneous data communication, defect inspection, and power transmission," IEEE Transactions on Ultrasonics, Ferroelectrics, and Frequency Control, vol. 68, no. 10, pp. 3192–3203, 2021.
7. M. Mälzer, C. Kexel, T. Maetz, and J. Moll, "Combined inspection and data communication network for lamb-wave structural health monitoring," IEEE Transactions on Ultrasonics, Ferroelectrics, and Frequency Control, vol. 66, no. 10, pp. 1625–1633, 2019.
8. C. Kexel, T. Maetz, M. Mälzer, and J. Moll, "Ultrasonic data transmission across metal structures affected by environmental conditions," Journal of Sound and Vibration, vol. 490, p. 115691, 2021.
9. S. M. Shaik, X. Tang, and S. Mandal, "Self-optimizing wireless networks on structures," IEEE Transactions on Circuits and Systems II: Express Briefs, vol. 67, no. 5, pp. 911–915, 2020.
10. C. Kexel, N. Testoni, F. Zonzini, J. Moll, and L. De Marchi, "Low-power mimo guided-wave communication," IEEE Access, vol. 8, pp. 217 425–217 436, 2020.
11. J. Wu, S. Yuan, X. Zhao, Y. Yin, and W. Ye 2007. "A wireless sensor network node designed for exploring a structural health monitoring application," Smart materials and structures, vol. 16, no. 5
12. S. Mustapha, Y. Lu, C.-T. Ng, and P. Malinowski, "Sensor networks for structures health monitoring: placement, implementations, and challenges—a review," Vibration, vol. 4, no. 3, pp. 551–585, 2021.
13. Mohammadgholiha, M., Palermo, A., Testoni, N., Moll, J., & De Marchi, L. (2022). "Finite element modeling and experimental characterization of piezoceramic frequency steerable acoustic transducers," IEEE Sensors Journal, 22(14), 13958-13970.
14. Moll, J. ; Kathol, J.; Fritzen, C.-P.; Moix-Bonet, M.; Rennoch, M.; Koerdt, M.; Herrmann, A.; Sause, M. & Bach, M., Open Guided Waves - Online Platform for Ultrasonic Guided Wave Measurements, Structural Health Monitoring (SAGE), 2019, Vol. 18(5-6), pp. 1903-1914
15. Zima, B., Reyes, O. A. M., Mohammadgholiha, M., Moll, J., & De Marchi, L. (2023). Data Compression in Ultrasonic Network Communication via Sparse Signal Processing. International Journal of Structural and Construction Engineering, 17(2), 98-104.
16. O. A. M. Reyes, B. Zima, J. Moll, M. Mohammadgholiha, and L. de Marchi, "A numerical study on baseline-free damage detection using frequency steerable acoustic transducers," in European Workshop on Structural Health Monitoring. Springer, 2023, pp. 24–33.
17. Moll, J. ; Kexel, C.; Kathol, J.; Fritzen, C.-P.; Moix-Bonet, M.; Willberg, C.; Rennoch, M.; Koerdt, M. & Herrmann, A., Guided waves for damage detection in complex composite structures: The influence of omega stringer and different reference damage size, Applied Sciences (Special Issue: "Guided Wave-Based Damage Identification for Composite Structures"), 2020, Vol. 10(9), 3068